Increase in Thrust of Magneto Plasma Sail Using Solid or Deployable Superconducting Coil

IEPC-2015-328／ISTS-2015-b-328

Presented at Joint Conference of 30th International Symposium on Space Technology and Science 34th International Electric Propulsion Conference and 6th Nano-satellite Symposium, Hyogo-Kobe, Japan July 4 – 10, 2015

Yoh Nagasaki[1]
Kyoto University, Nishikyo, Kyoto, 615-8510, Japan

Ikkoh Funaki[2]
Japan Aerospace Exploration Agency, Sagamihara, Kanagawa 252-5210, Japan

and

Taketsune Nakamura[3] and Hiroshi Yamakawa[4]
Kyoto University, Nishikyo, Kyoto, 615-8510, Japan

Abstract: This study designed a light-weight High Temperature Superconducting (HTS) coil with a larger magnetic moment and investigated the feasibility of a deployable coil for a magneto plasma sail. For the optimal design of the HTS coil for use in space, we analyzed the nonlinear current transport characteristics, thermal stabilities, and applied mechanical stresses of HTS coils on the basis of a developed thermo-electromagnetic analysis method with taking into account radiation cooling condition. Using the genetic algorithm and developed analysis method, we optimized the configuration of the HTS coil at a specific constraint condition of the magneto plasma sail system to obtain as large magnetic moment to mass ratio as possible. As an optimization result, we showed that a thin-walled racetrack coil with a larger diameter can achieve a magnetic moment at 2.6×10^7 Am^2 which were five times larger than that obtained from a previous study. We also simulated a coil deployment using an electromagnetic force applied to the coil during the excitation of the coil. The simulation result showed that a coil stored in the spacecraft can be successfully deployed using the electromagnetic force without deployment structures. This study proves the possibility of greatly increasing the thrust to mass ratio of the magneto plasma sail.

Nomenclature

B	=	magnetic field
B_x	=	X component of the magnetic field
B_y	=	Y component of the magnetic field
θ	=	magnetic field direction
C	=	specific heat capacity
κ	=	thermal conductivity
t	=	time
E	=	electric field

[1] Ph. D. candidate, Electrical Engineering, nagasaki@rish.kyoto-u.ac.jp
[2] Associate Professor, Institute of Space and Astronautical Science, funaki.ikkoh@jaxa.jp
[3] Associate Professor, Electrical Engineering, tk_naka@kuee.kyoto-u.ac.jp
[4] Professor, Electrical Engineering, yamakawa@rish.kyoto-u.ac.jp

$\boldsymbol{F}$	=	electromagnetic force
I	=	operational transport current
I_c	=	critical current
J	=	current density
J_{cm}	=	minimum value of a local critical current density distribution
J_0	=	scaling factor describing the width of a local critical current density distribution
l	=	layer number of the coil
m	=	statistical parameter characterizing the shape of a local critical current density distribution
N	=	total turn number of the coil
n	=	stack number of the coil
s	=	coil element
$\boldsymbol{r}$	=	position vector for each coil element s
r_o	=	outside radius
r_l	=	radius for layer l
S	=	area enclosed by the coil
T	=	temperature
T_{op}	=	operational temperature
μ	=	magnetic moment
ρ_{FF}	=	resistivity for uniform flux flow.
ρ	=	line density
σ	=	local tensile force

I. Introduction

Superconducting coils can revolutionize space propulsion systems [1-8]. The performances, e.g., acceleration and thrust to power ratio, of a magneto plasma sail can be greatly improved with a superconducting coil by generating a larger magnetic field with less power consumption and weight. The magneto plasma sail is a spacecraft propulsion system with higher specific impulse for future deep space explorations [1, 3, 4]. Figure 1 shows the conceptual diagram of the magneto plasma sail. The thrust of the magneto plasma sail is produced by the interaction between a solar wind plasma and a strong magnetic field generated by a High Temperature Superconducting (HTS) coil installed in the spacecraft. The magneto plasma sail forms a stronger magnetic field using plasma jets from the spacecraft as well as an HTS coil as shown in Fig. 1.

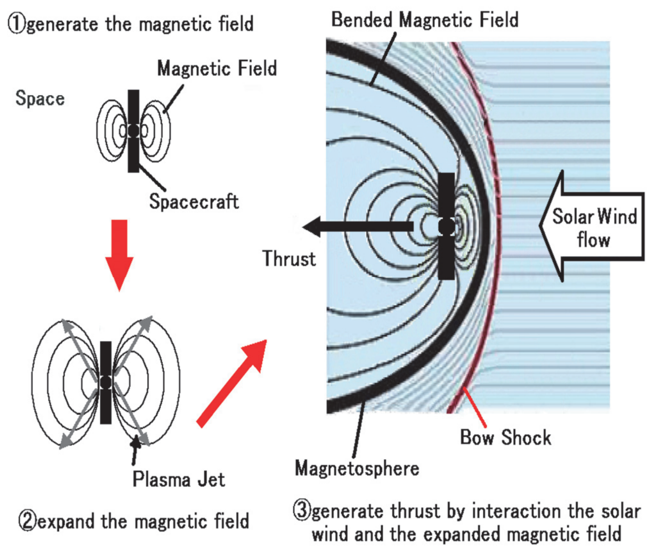

Figure 1. Concept of the magneto plasma sail.

The propulsive force is proportional to the magnetic moment, μ, of the installed coil. In order to obtain an adequate driving force, a magnetic moment, $\mu = SNI$, to mass ratio of the coil must be improved as large as possible. S denotes the area enclosed by the coil and NI (N: total turn number of the coil, I: operational transport current) is the magnetomotive force of the coil. One method to increase the magnetic moment is to enlarge S. Spacecraft size, however, is typically limited to be less than φ4 m due to the installation size limit in the rocket for launch. Another way to increase μ is to enlarge NI. HTS coils have a big advantage for increasing I, and this is one of the major motivations to utilize the HTS coil for the magneto plasma sail.

In order to obtain an enough thrust to mass ratio, or acceleration, for space missions and realize the magneto plasma sail, the magnetic moment to mass ratio of the installed HTS coil must be drastically increased. We have two approaches for this purpose. The first approach is to optimize the HTS coil to increase the coil current and maximize its magnetic moment within the capacity of a space vehicle. The second approach is to develop a deployable superconducting coil with a larger diameter and increase the coil area and magnetic moment by deploying the coil in space. We aim for a light-weight HTS coil system based on radiation and/or cryocooler cooling, following the JAXA SPICA satellite [9]. The HTS coil must be designed with a larger magnetic moment and higher thermal stability without the use of any refrigerants.

Since the magneto plasma sail requires a large-sized coil with a diameter of more than 4 m, electromagnetic forces such as a hoop stress applied to the coil becomes a serious constraint on the design of the coil. Yttrium Barium Copper Oxide (YBCO)–coated conductors (CCs) are expected to be utilized in larger-sized coils than in the case of Bi-2223, due to the high tolerance of Hastelloy® substrates. In this study, the HTS coil using YBCO CCs was designed for the magneto plasma sail. The electromagnetic force applied to the coil as well as the thermal stability were considered to avoid the degradation of superconducting properties in space.

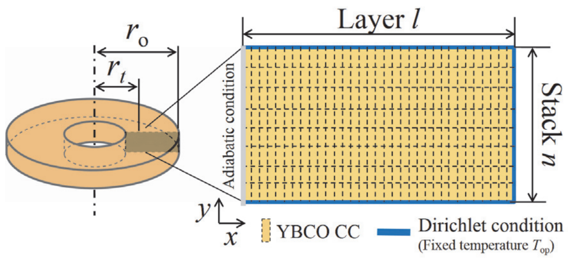

Figure 2. Schematic diagram of a cross-section of an analyzed YBCO coil.

In this paper, we analyzed the current transport performance, the thermal stability, and the applied stresses of YBCO coils with a variety of coil configurations, such as circular, multi pole or racetrack coils, on the basis of an electromagnetic field as well as thermal analysis. The configuration of the coil was optimized using genetic algorithm to maximize the magnetic moment, μ, to mass ratio of the coil, based on the constraint conditions of the thermal stability, hoop stress, transverse compressive stress in the coils. A coil deployment using an electromagnetic force was also simulated to demonstrate the feasibility of the light-weight deployment system for an HTS coil.

II. Design of Solid Coil

A. Analysis Method

Figure 2 illustrates the analysis model of a designed coil. Since the coil is cooled by radiation in outer space, the boundary conditions for the temperature is set as shown in Fig. 2. The Dirichlet condition (constant temperature T_{op}) is set at the top, bottom, and outer surfaces of the coil and the Adiabatic condition on the inner surface. YBCO CCs for the winding were 3.0 mm wide and 0.1 mm thickness and additionally reinforced with Hastelloy® tapes. We analyze the current transport property of the HTS coil with considering the distributed magnetic field, temperature and electric field in the coil using a thermo-electromagnetic field analysis [10, 11] based on the percolation depinning model [12-14]. The electric field, E, versus current density, J, characteristics of HTS tapes can be described as functions of temperature, T, magnetic field, B, and its applied direction, θ, from the following percolation depinning model[12-14]:

$$E = \begin{cases} \dfrac{\rho_{FF} J_0(T,B,\theta)}{m+1}\left(\dfrac{J - J_{cm}(T,B,\theta)}{J_0(T,B,\theta)}\right)^{m+1} \\ \text{for } 0 \le J_{cm} \\ \dfrac{\rho_{FF} J_0(T,B,\theta)}{m+1}\left[\left(\dfrac{J + |J_{cm}(T,B,\theta)|}{J_0(T,B,\theta)}\right)^{m+1} - \left(\dfrac{|J_{cm}(T,B,\theta)|}{J_0(T,B,\theta)}\right)^{m+1}\right], \\ \text{for } 0 > J_{cm} \end{cases} \quad (1)$$

where ρ_{FF} is the resistivity for uniform flux flow. J_{cm}, J_0, and m denote the minimum value, the scaling factor describing the width, and the statistical parameter characterizing the shape of a local critical current density distribution, respectively. The magnetic field, B, is calculated using the Biot-Savart law.

The thermal stability of the coil is analyzed calculating heat generation per unit volume $J \cdot E$ and solving the heat balance equation as described below.

$$C\frac{\partial T}{\partial t} = \frac{\partial}{\partial x}\left\{\kappa \frac{\partial T}{\partial x}\right\} + \frac{\partial}{\partial y}\left\{\kappa \frac{\partial T}{\partial y}\right\} + J \cdot E \quad (2)$$

where C denotes specific heat capacity, κ thermal conductivity and t time. The x–y plane in the equation is the cross section of the coil described in Fig. 2. The initial temperature is set to 20 K. The temperature inside of the coil is calculated at a fixed operational current value until the temperature diverges or converges to a specified temperature.

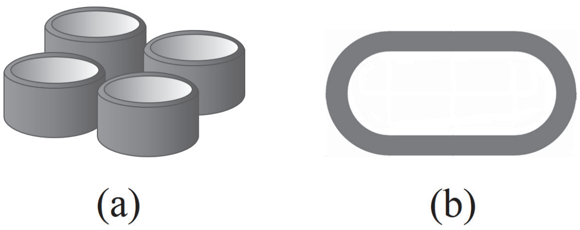

Figure 3. (a) multi-pole and (b) racetrack coil

We finally obtain the time transient of the coil temperature with fixed current values and the maximum operational current I_c for the HTS coil in terms of the thermal stability.

B. Design Constraints

By using the developed analysis method, the configuration of the coil is optimized to maximize the magnetic moment to mass ratio of the coil, i.e. the acceleration of the magneto plasma sail. We now analyze three kinds of the coil configurations; circular, multi-pole, and racetrack coil shown in Fig. 3. The multi-pole coil consists of more than one coil and the racetrack coil is the coil with the racetrack geometry. The outside radius, r_o, the number of layers, l, and stack, n, of the coils are optimized using the genetic algorithm in order to maximize the magnetic moment to mass ratio.

The magnetic moment, μ, of the circular coil is calculated from the following equation.

$$\mu = \sum_{t=1}^{N} I \pi r_t^2 \qquad (3)$$

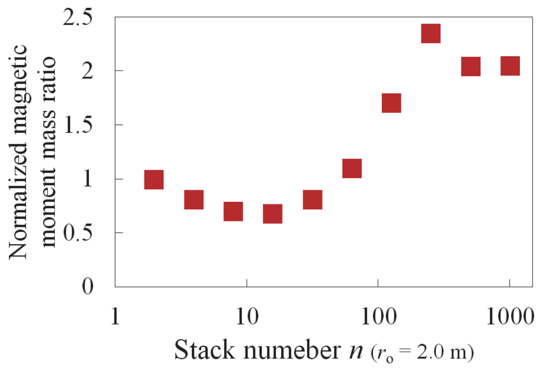

Figure 4. Normalized magnetic moment to mass ratio of circular coils with a variety of stack numbers. The outside radius r_o = 2.0 m and the total length of the YBCO CCs is constant.

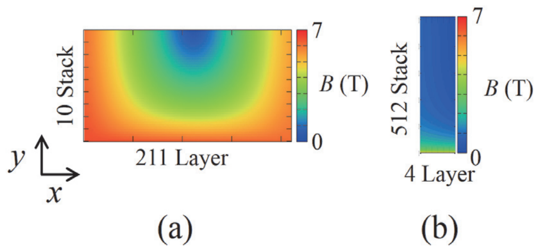

Figure 5. Magnetic flux density distribution in the cross section of coils. (a) 211 layer, 20 stack (aspect ratio is around 1:1), (b) 4 layer, 1024 stack. Only the lower half of the coil cross section is described due to the symmetry of the electromagnetic field in the coil.

The total turn number N is obtained from $m \times n$. The operational current I for the coil is determined when the analysis meets the following conditions.

1. The coil temperature T diverges.
2. Hoop stresses applied to the coil, which are calculated as $B_y \times J \times r_t$[15] at each turn t, exceed 1 GPa.
3. Transverse compressive stresses applied to the coil exceed 150 MPa.

The YBCO CCs tolerate this level of stress in term of the mechanical strength [16-18]. The thickness of the Hastelloy® substrates is adjusted according to the applied stresses to the coil. We also consider the constraint conditions described below:

4. Coil size is limited to φ 4 m × 7 m, due to the installation size limitation in the rocket for launch.

The optimal configuration of the coil is determined by evaluating the magnetic moment and the constraint parameters on each coil design.

C. Results and Discussion

We first performed sensitivity analyses using the method explained in the previous section with changing the geometry parameters of the coil. Figure 4 indicates the relationship between the stack number, n, in the case of r_o = 2.0 m, and the magnetic moment to mass ratio of circular coils. The total length of the YBCO CCs is constant, approximately 50 km. The magnetic moment to mass ratio is normalized by that of an HTS coil offered by a former

Table 1: Optimal designs for each coil configuration.

	Circular	Multi-pole	Racetrack
Weight	200 kg	200 kg	200 kg
$2r_o$	4.0 m	4.0 m	3.8 m × 7.0 m
n	585 stack	250 stack	453 stack
l	7 layer	4 layer	6 layer
I	526 A	606 A	635 A
NI (A-turns)	1.1×10^6	3.7×10^6	1.2×10^6
Normalized magnetic moment to mass ratio	3.7	4.1	5.5

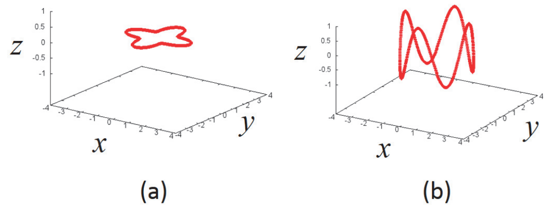

Figure 6. Coil (a) folded in the radial direction, and (b) folded in the axial direction.

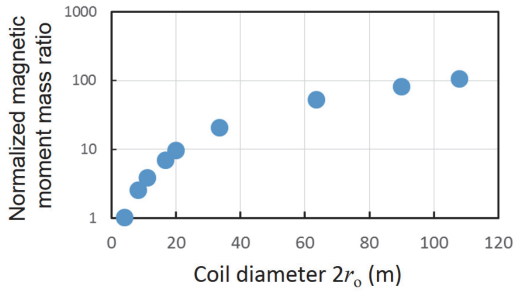

Figure 7. Normalized magnetic moment to mass ratio of circular coils with a variety of coil diameter. The total length of the YBCO CCs is constant.

study (the maximum operational current: 200 A, diameter: 3.5 m, 211 layer × 20 stack, 200 kg). As can be seen in Fig. 4, the magnetic moment to mass ratio increases with a higher stack number n, or, in other words, a lower layer number m. On the other hand, the magnetic moment to mass ratio decreases when the aspect ratio of the cross section of the coil is around 1:1 (n = 15). This is because the maximum operational current I_c increases with a higher stack number and decreases with the aspect ratio of 1:1 due to the magnetic flux density in the coils as shown in Fig. 5. The superconducting property in a higher magnetic field region is deteriorated because of the magnetic field dependency of the E–J characteristics of the HTS tapes.

As can also be seen in Fig. 4, the magnetic moment to mass ratio decreases in a very high stack number. This is because the transverse compressive stress increases with the decreasing top and bottom surface areas of the coil, i.e., with the increasing n and decreasing m, and exceeds the upper limit (150 MPa) for the YBCO CCs in those configurations.The sensitive analysis results show that the magnetic moment to mass ratio largely depends on the coil configuration. Using the genetic algorithm, we optimized the coil configuration to obtain the maximum magnetic moment to mass ratio for three kinds of the coils. Table. 1 shows the optimal configurations of circular, multi-pole, racetrack coil under the specific constraint conditions, respectively. The optimization results reveal that the racetrack coil can maximize the magnetic moment to mass ratio which is 5.5 times larger than that of the previous study. For the racetrack coil, both of the operational current and the area of the racetrack coil can be larger than those of the circular coil, considering the thermal stability and installation size limitation in the rocket. We successfully improved the magnetic moment to mass ratio of the coil by optimizing the configuration of the coil in terms of the thermal stability and applied electromagnetic force. However, our goal is to use HTS conductors to realize the magnetomotive force $NI = 10^7$ A-turns or the magnetic moment $\mu = 1.2\times10^8$ A·m^2, which is almost 10 times larger than the result of this study. We next consider the feasibility of the coil deployment system in space in order to increase the area enclosed by the coil.

III. Deployable Coil

We investigated the feasibility of a deployable coil to drastically increase the magnetic moment of the coil. A coil with a diameter of more than 4 m folded in the radial or axial direction (as shown in Fig. 6) and stored in the rocket is deployed in space after the launch to increase the area enclosed by the coil and magnetic moment. We firstly optimized circular HTS coils with a diameter of from 2 m to 110 m in order to investigate the dependence of the magnetic moment on the coil diameter. Figure 7 shows the relationship between the coil diameter and magnetic moment to mass ratio of the coil obtained from the optimization. As shown in the figure, the magnetic moment to mass ratio drastically increases with the coil diameter. This is because with the increasing coil diameter, the coil surface area, that is cooling surface area, increases and, as a result, thermal stability improves. Due to the increasing coil area and thermal stability, the magnetic moment can be greatly improved with the increasing coil diameter.

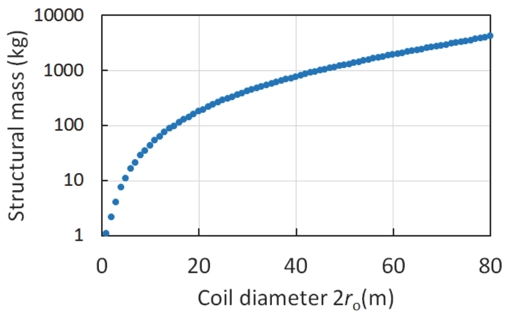

Figure 8. Total weight of the deployment structure for a variety of coil diameter after the deployment.

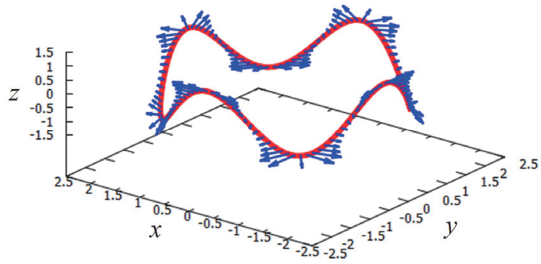

Figure 9. Electromagnetic force distribution. (red line: a folded coil, blue arrows: electromagnetic force vectors)

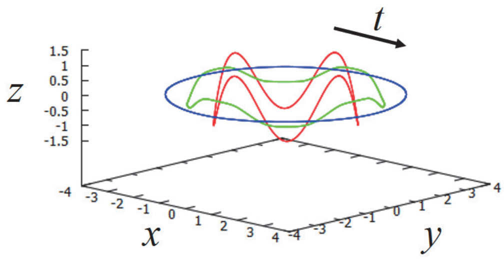

Figure 10. Simulation result of a coil deployment with an electromagnetic force. (red line: original position, blue line: after deployment)

Figure 7 also indicates that the deployable coil with a diameter of 20 m can achieve the magnetic moment which is ten times larger than that of the previous study.

As a method for the coil deployment, using an extensible beam or some support structure might be applied. However, to obtain an enough thrust from the magneto plasma sail for space missions, large scale structure such as a diameter of more than 20 m is required. Figure 8 shows that the relationship between the coil diameter and the total weight of the deployment system using an extensible beam. We assumed the extensible beam made of Aluminum (Density: 2.7 g/cm^3). As shown in Fig. 8, a deployable coil with a diameter of 20 m needs a deployment structure weighing up to 200 kg. As can also be seen in Fig. 8, as the coil diameter increases, the weight of the required system greatly increases to more than 1000 kg since the coil with a larger diameter needs a larger number of the extensible beams.

In this study, we investigated one possible method for a coil deployment in space using an electromagnetic force to reduce the weight of the system and increase the magnetic moment to mass ratio. During the coil excitation, an electromagnetic force between the coil current and coil magnetic field, which is so-called hoop stress, acts on the coil in radial direction. Figure 9 describes the distribution of the electromagnetic force acting on a coil folded in the axial direction during the excitation. As can be seen in Fig. 9, the electromagnetic force acts to the outer direction to which the coil expands. The coil deployment using the electromagnetic force was also proposed for a deployment of a space telescope [19]. The coil is folded and stored during launch and can be deployed in space without any deployment structure by using such electromagnetic force.

We simulated the coil deployment using the electromagnetic force by solving the equation of motion described below.

$$\rho \frac{\partial^2 \boldsymbol{r}}{\partial t^2} = \frac{\partial}{\partial s}\left(\sigma \frac{\partial \boldsymbol{r}}{\partial s}\right) + \boldsymbol{F}, \quad \frac{\partial \boldsymbol{r}}{\partial s} \cdot \frac{\partial \boldsymbol{r}}{\partial s} = 1 \tag{3}$$

where $\boldsymbol{r}$ denotes the position vector for each coil element s, $\boldsymbol{F}$ electromagnetic force, t time, ρ line density, σ local tensile force, respectively. For the simplicity, the motion of one turn coil was analyzed in a free space.

Figure 10 describes the time transient of the coil deployment as a simulation result. The inner line shows the initial coil shape, and outer line shows the shape after the deployment. As shown in the figure, we confirmed that the folded coil were successfully deployed with the electromagnetic force. Our future work is to conduct a structural analysis as well as verify the coil deployment using the electromagnetic force by conducting a current and deployment test.

IV. Conclusion

This study designed the optimal solid HTS coil for the magneto plasma sail and also investigated the feasibility of a deployable coil to increase the magnetic moment of the coil and thrust of the magneto plasma sail. From a point of view of maximizing the magnetic moment to mass ratio of the solid HTS coil, a racetrack coil with a thin-wall is the optimal configuration, and the magnetic moment to mass ratio can be increased to 5 times larger than that of a former study. This paper also demonstrated the feasibility of the deployable coil using an electromagnetic force by a numerical simulation. Verifying the simulation results by an experiment and developing a cooling and power system for the magneto plasma sail are our future work. With taking into account the total weight of the spacecraft system, we will design an HTS coil system to obtain an enough magnetic moment to mass ratio for future deep space explorations.

Acknowledgments

This work was supported in part by the engineering committee of the Institute of Space and Astronautical Science of the Japan Aerospace Exploration Agency and by a Grant-in-Aid for JSPS Fellows.

References

[1] R. M. Zubrin, and D. G. Andrews, "Magnetic sails and interplanetary travel," *J. Spacecraft Rockets,* vol. 28, no. 2, pp. 197-203, Mar-Apr, 1991.

[2] G. Vulpetti, "A critical-review on the viability of a space propulsion based on the solar-wind momentum flux," *Acta Astron.,* vol. 32, no. 9, pp. 641-644, Sep, 1994.

[3] R. M. Winglee, J. Slough, T. Ziemba, and A. Goodson, "Mini-magnetospheric plasma propulsion: Tapping the energy of the solar wind for spacecraft propulsion," *J. Geophys. Res.,* vol. 105, no. A9, pp. 21067-21077, Sep 1, 2000.

[4] H. Yamakawa, I. Funaki, Y. Nakayama, K. Fujita, H. Ogawa, S. Nonaka, H. Kuninaka, S. Sawai, H. Nishida, R. Asahi, H. Otsu, and H. Nakashima, "Magneto-plasma sail: An engineering satellite concept and its application for outer planet missions," *Acta Astron.,* vol. 59, no. 8-11, pp. 777-784, Oct-Dec, 2006.

[5] C. Bruno, and S. Giucci, "Cryogenic technology to improve electric thrusters," *Acta Astron.,* vol. 51, no. 12, pp. 855-863, Dec, 2002.

[6] C. Bruno, and D. Casali, "Superconducting materials applied to electric propulsion systems," *J. Spacecraft Rockets,* vol. 41, no. 4, pp. 671-676, Jul-Aug, 2004.

[7] C. M. Rey, W. C. Hoffman, F. R. Chang-Diaz, A. V. Ilin, A. J. Petro, D. S. Winter, H. Mukai, and S. W. Schwenterly, "Design and fabrication of an HTS magnet for the VASIMR experiment," *IEEE Trans. Appl. Supercond.,* vol. 12, no. 1, pp. 993-996, Mar, 2002.

[8] Y. Wang, B. Li, P. Zhang, and S. Wang, "Magnet configuration and experimental analysis of helicon source for space magnetoplasma propulsion," *IEEE Trans. Appl. Supercond.,* vol. 20, no. 3, pp. 993-996, 2010.

[9] H. Sugita, T. Nakagawa, H. Murakami, A. Okamoto, H. Nagai, M. Murakami, K. Narasaki, and M. Hirabayashi, "Cryogenic infrared mission "JAXA/SPICA" with advanced cryocoolers," *Cryogenics,* vol. 46, no. 2-3, pp. 149-157, 2006.

[10] Y. Nagasaki, T. Nakamura, I. Funaki, Y. Ashida, and H. Yamakawa, "Coupled-analysis of current transport performance and thermal behaviour of conduction-cooled Bi-2223/Ag double-pancake coil for magnetic sail spacecraft," *Phys. C, Supercond.,* vol. 492, pp. 96-102, Sep, 2013.

[11] Y. Nagasaki, T. Nakamura, I. Funaki, Y. Ashida, and H. Yamakawa, "Numerical Investigation on Thermal Stability of Conduction-Cooled Bi-2223/Ag Coil Under AC Ripple Current for Space Applications," *IEEE Trans. Appl. Supercond.,* vol. 24, no. 3, pp. 1-5, 2014.

[12] T. Kiss, M. Inoue, T. Kuga, M. Ishimaru, S. Egashira, S. Irie, T. Ohta, K. Imamura, M. Yasunaga, M. Takeo, T. Matsushita, Y. Iijima, K. Kakimoto, T. Saitoh, S. Awaji, K. Watanabe, and Y. Shiohara, "Critical current properties in HTS tapes," *Phys. C, Supercond.,* vol. 392-396, pp. 1053-1062, 2003.

[13] K. Yamauchi, M. Kiuchi, E. S. Otabe, T. Matsushita, T. Kuga, M. Inoue, T. Kiss, Y. Iijima, K. Kakimoto, and T. Saitoh, "Evaluation of E–J characteristics of YBCO-coated conductor in a wide range of electric field," *Physica C: Superconductivity,* vol. 392–396, Part 2, no. 0, pp. 1073-1077, 10//, 2003.

[14] T. Nakamura, S. Tsuchiya, A. Fujio, T. Hoshino, I. Muta, and M. Yamaguchi, "Angular dependence of E-J characteristics and dissipative properties in Bi-2223/Ag tape," *Supercond. Sci. Technol.,* vol. 15, no. 2, pp. 230-235, Feb, 2002.

[15] A. Otsuka, and T. Kiyoshi, "High-field magnet design under constant hoop stress," *IEEE Trans. Appl. Supercond.,* vol. 18, no. 2, pp. 1529-1532, Jun, 2008.

[16] M. Sugano, T. Nakamura, K. Shikimachi, N. Hirano, and S. Nagaya, "Stress tolerance and fracture mechanism of solder joint of YBCO coated conductors," *IEEE Trans. Appl. Supercond.,* vol. 17, no. 2, pp. 3067-3070, Jun, 2007.

[17] M. Sugano, Y. Yoshida, M. Hojo, K. Shikimachi, N. Hirano, and S. Nagaya, "Two different mechanisms of fatigue damage due to cyclic stress loading at 77 K for MOCVD-YBCO-coated conductors," *Supercon. Sci. Technol.,* vol. 21, no. 5, pp. 054006, 2008.

[18] N. Cheggour, J. W. Ekin, C. L. H. Thieme, and Y.-Y. Xie, "Effect of fatigue under transverse compressive stress on slit Y-Ba-Cu-O coated conductors," *IEEE Trans. Appl. Supercond.,* vol. 17, no. 2, pp. 3063-3066, Jun, 2007.

[19] G. V. Gettliffe, "High-Temperature Superconductors as Electromagnetic Deployment and Support Structures in Spacecraft," 2013.